

Promotion of Reductive Elimination Reaction of Diorgano(2,2'-bipyridyl)nickel(II) Complexes by Electron-Accepting Aromatic Compounds, Lewis Acids, and Brønsted Acids.

Takakazu Yamamoto,* Mahmut Abla, and Yasuharu Murakami

Chemical Resources Laboratory, Tokyo Institute of Technology, 4259 Nagatsuta, Midori-ku, Yokohama 226-8503

(Received March 13, 2002)

Reductive elimination of R-R from dialkyl(2,2'-bipyridyl)nickel(II), [NiR₂(bpy)] **1** (R = CH₃ (**1a**), C₂H₅ (**1b**), *n*-C₃H₇ (**1c**)), caused by π -coordination of electron-accepting aromatic compounds and reductive elimination of Ar-Ar from [NiAr₂(bpy)] **2** (Ar = C₆F₅ (**2a**) and pyrazolyls (**2b** and **2c**)) promoted by electron-accepting aromatic compounds, Lewis acids, and Brønsted acids have been investigated. ¹H-NMR and kinetic data indicate that π -coordination of the electron-accepting aromatic compound to [NiR₂(bpy)] leads to the reductive elimination of R-R. The rate of the reductive elimination obeys the second-order rate law, $-d[\mathbf{1}]/dt = k[\mathbf{1}][\text{electron-accepting aromatic compound}]$. Plots of $\log k$ vs $\Sigma\sigma_p$ of the electron-accepting aromatic compound give a line with a slope of 1.8. Brønsted acids cause reductive elimination of Ar-Ar from **2** selectively under several reaction conditions (e.g., **2a** with CF₃COOH in air and **2b** with HBr). The reductive elimination reaction of **2a** caused by CF₃COOH obeys the second-order rate law, $-d[\mathbf{2a}]/dt = k'[\mathbf{2a}][\text{CF}_3\text{COOH}]$, in air. The reaction of **2b** with H₂SO₄ requires O₂, giving the rate equation, $-d[\mathbf{2b}]/dt = k''[\mathbf{2b}]^2[\text{O}_2]$; k'' increases with [H₂SO₄], reaching a maximum value at a high [H₂SO₄]. UV-vis spectroscopy reveals the presence of the following equilibrium: **2b** + H₂SO₄ \rightleftharpoons **2b**·H₂SO₄, and the equilibrium constant K_a is evaluated as $K_a = [\mathbf{2b}\cdot\text{H}_2\text{SO}_4]/([\mathbf{2b}][\text{H}_2\text{SO}_4]) = 47 \text{ M}^{-1}$ at 300.5 K. UV-vis data give information about the electronic states of **2** and the **2b**-Brønsted acid adduct. Poly(6-hexylpyridine-2,5-diyl) with a higher molecular weight has been prepared according to the basic information.

Reductive elimination is one of the most fundamental reactions in organometallic chemistry.¹⁻⁴ The reductive elimination of Y-Y' from [Ni(Y)(Y')L_n] and [Pd(Y)(Y')L_n] (Y, Y' = organic group) is considered to be a key step in Ni- and Pd-complex promoted organic synthesis^{1,5,6} and polymer synthesis.^{7,8}

Factors that control the reductive elimination from diorganometallic complexes, [M(Y)(Y')L_n] (M = Ni, Pd; L = neutral ligand such as 2,2'-bipyridyl and tertiary phosphines) have long been investigated.¹⁻³

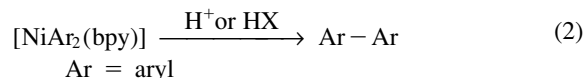


However, there still remain unclarified factors concerning the reductive elimination.

A few papers have been published on the reductive elimination reaction of [Ni(alkyl)₂L_n]^{2a-g} and [Ni(alkyl)(aryl)L_n].^{2h} However, little attention has been paid to the reductive elimination reaction of [Ni(aryl)₂L_n], presumably due to the presence of significantly fewer examples of isolated [Ni(aryl)₂L_n].⁹ The diaryl nickel complex has been isolated mainly with electron-withdrawing aryl groups that stabilize the Ni-aryl bond.

In this paper, we report details of (i) the reductive elimination reaction of [Ni(alkyl)₂(bpy)] (bpy = 2,2'-bipyridyl) accelerated by the coordination of electron-accepting aromatic compounds such as *m*- and *p*-C₆H₄(CN)₂ and (ii) the reductive elimination reaction of [Ni(aryl)₂(bpy)] induced by Lewis acid and protic acids. The Brønsted acids usually induce the cleav-

age of metal-organic (M-Y) bonds to liberate Y-H compounds;^{1,3c,9f,10} however, the present investigation reveals that it can cause selective reductive elimination when the organic group is the electron-accepting aryl group.



Analysis of these reductive elimination reactions is expected to improve our understanding of the nickel-complex-promoted synthetic reactions. A part of these results have been published in a communication form.^{9c-e}

Results and Discussion

Reductive Elimination and UV-Vis Data of Diorganonickel(II) Complex. Tables 1 and 2 summarize the results of the reductive elimination of [Ni(alkyl)₂(bpy)], [NiR₂(bpy)] **1**, and [Ni(aryl)₂(bpy)], [NiAr₂(bpy)] **2**, caused by various accelerating reagents. Diorgano(2,2'-bipyridyl)nickel(II) complexes, [NiY₂(bpy)], with the alkyl and aryl groups shown in Chart 1, are used in this study.

Structure of [NiAr₂(bpy)]. The molecular structures of complexes **2a**, **2b**, and **2c**^{9c} have been determined by X-ray crystallography; they take a square planar structure around Ni, as previously reported for **2c**. The molecular structure of **2a** is shown in Figure 1 and that of **2b** is given in the supporting data.

Reductive Elimination from [NiR₂(bpy)]. As shown in

Table 1. Results of the Reductive Elimination of [NiR₂(bpy)] and [NiAr₂(bpy)] (R = Alkyl, Ar = Aryl) Promoted by Electron-Accepting Aromatic Compounds and Lewis Acids

Run	R or Ar, complex	Accelerating reagent ^{a)}	Solvent ^{b)}	Temp/°C	Yield of R-R or Ar-Ar/% ^{c)}
1	Me (1a)	<i>m</i> -C ₆ H ₄ (NO ₂) ₂	THF	r.t.	95
2	1a	C ₆ H ₅ NO ₂	THF	r.t.	93
3	1a	C ₆ F ₅ CF ₃	THF	r.t.	84
4	Et (1b)	<i>m</i> -C ₆ H ₄ (NO ₂) ₂	THF	r.t.	87
5	1b	<i>p</i> -C ₆ H ₄ (CN) ₂	THF	r.t.	93
6	1b	<i>o</i> -C ₆ H ₄ (CN) ₂	THF	r.t.	96
7	1b	C ₆ H ₅ CN	THF	r.t.	81
8	Pr (1c)	<i>m</i> -C ₆ H ₄ (NO ₂) ₂	THF	r.t.	100
9	1c	<i>o</i> -C ₆ H ₄ (CN) ₂	THF	r.t.	100
10	1c	C ₆ H ₅ CF ₃	THF	r.t.	97
11	1c	C ₆ F ₆	THF	r.t.	93
12	1c	1,3,5-C ₃ H ₃ N ₃	THF	r.t.	90
13	1c	1,4-C ₄ H ₄ N ₂	THF	r.t.	89
14	C ₆ F ₅ (2a)	acrylonitrile	DMSO or DMF	70	0 ^f
15	2a	acrylonitrile	toluene	reflux	0
16	2a	maleic anhydride	DMSO	100	trace
17	2a	TCNE	toluene	reflux	0
18	2a	TCNQ	toluene	105	100
19	C ₃ N ₂ (CH ₃) ₂ Cl (2b)	C ₆ F ₆	CH ₃ CN	50	3
20	2b	maleic anhydride	CH ₃ CN	50	66
21	2b	TCNE	CH ₃ CN	50	44
22	2b	TCNQ	CH ₃ CN	50	94
23	C ₃ N ₂ (CH ₃)COOMeCl (2c)	TCNQ	CH ₃ CN	r.t.	89
Accelerating reagent = Lewis acid					
24	2b	BF ₃ ·OEt ₂	CHCl ₃	30	28
25	2b	RuCl ₃ ^{d)}	CHCl ₃ ^{e)}	30	82

a) 1,3,5-C₃H₃N₃ = 1,3,5-triazine. 1,4-C₄H₄N₂ = pyrazine. TCNE = tetracyanoethylene. TCNQ = tetracyanoquinodimethane. An excess amount of the accelerating reagent (about 10 mol/1 mol of the Ni complex) was added. b) DMSO = dimethyl sulfoxide. DMF = *N,N*-dimethylformamide. c) GLC yield. A trace amount of RH (methane) was detected in run 3. A part of the gaseous product (C₂H₆ or butane) may be lost during the reaction, whereas the liquid product (hexane) from **1c** should remain in the reaction solution. d) Hydrated (RuCl₃·*n*H₂O, *n* = ca. 3). e) In a dispersion system.

alkyl = CH₃ (complex **1a**), C₂H₅ (complex **1b**), *n*-C₃H₇ (complex **1c**).

aryl = C₆F₅ (complex **2a**),

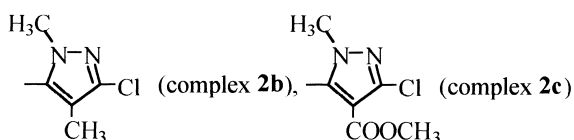
Chart 1. Organic groups in [NiY₂(bpy)] used in this study.

Table 1, the reductive elimination of R-R from [NiR₂(bpy)] (**1a–1c**) is caused by the interaction with electron-accepting aromatic compounds such as C₆H₅CN and C₆F₆, similar to that caused by electron-accepting olefins.^{1,3a,b} 1,3,5-triazine and pyrazine (runs 12 and 13 in Table 1) are also regarded as π -deficient aromatic compounds due to the presence of electron-withdrawing imine nitrogens,¹¹ and interaction with these heterocyclic aromatic compounds also induces the reductive elim-

ination reaction of **1c**. [NiR₂(bpy)] is stable in usual aromatic solvents such as benzene and toluene.

Stability of and Preparative Conditions for [NiAr₂(bpy)]. C₆F₅- is a typical electron-withdrawing group and the pyrazolyl groups in **2b** and **2c** are also regarded as electron-withdrawing groups because they contain the imine nitrogen¹¹ and Cl. Complexes **2a–2c** are prepared by the following reaction route (Scheme 1) that involves the oxidative addition¹² of aryl

Table 2. Results of the Brønsted Acid-Promoted Reductive Elimination of Ar-Ar from [NiAr₂(bpy)]

Run	Complex	HX ^{a)}	Atmosphere	Temp/°C	Yield/% ^{b)}	
					Ar-Ar	ArH
1	2a	CF ₃ COOH(1.1M)	air	r.t.	100	0
2	2a	CF ₃ COOH(neat)	N ₂	r.t.	0	50
3	2a	CF ₃ COOH(neat)	air	r.t.	95	0
4	2a	HCl(1.0 M)	air	100	100	0
5 ^{c)}	2a	HBr(1.3 M)	N ₂	r.t.	92	0
6	2b	HCl(0.3 M)	air	r.t.	29	67
7	2b	HCl(0.3 M)	O ₂	30	72	23
8	2b	HCl(0.3 M)	N ₂	50	0	100
9	2b	HBr(0.3 M)	air	30	100	0
10	2b	HBr(0.3 M)	N ₂	50	100	0
11	2b	HNO ₃ (0.3 M)	air	30	83	15
12	2b	HNO ₃ (0.3 M)	O ₂	30	90	5
13	2b	H ₂ SO ₄ (0.3 M)	air	30	69	31
14	2b	H ₂ SO ₄ (0.3 M)	air	70	69	31
15	2b	H ₂ SO ₄ (0.3 M)	O ₂	r.t.	90	10
16	2c	HNO ₃ (6.0 M)	air	r.t.	97 ^{d)}	0
17	2c	CH ₃ COOH	air	r.t.	81	0

a) In DMSO-*d*₆ except for runs 2, 3, and 16 (aqueous solution) and 17 (1:1 mixture of CH₃OH and CHCl₃). b) Determined by ¹H NMR or GLC unless otherwise noted. Reaction time = about 10 h. c) Reaction was almost completed in 30 min. d) Isolated yield. Carried out with aqueous solution under heterogeneous conditions.

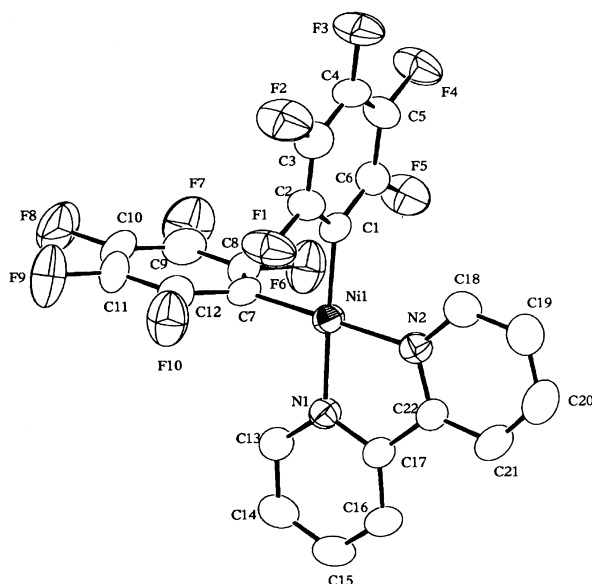
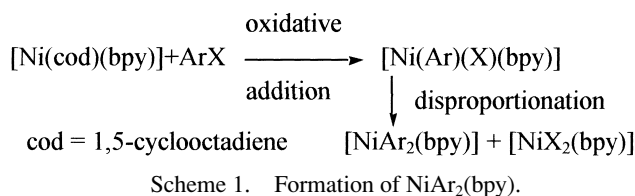


Fig. 1. Molecular structure of [Ni(C₆F₅)₂(bpy)] **2a**. Selected bond lengths (Å) and angles (deg): Ni–C1 1.903(4), Ni–C7 1.907(4), Ni–N1 1.938(3), Ni–N2 1.936(4), C1–Ni–C7 86.7(2), N1–Ni–N2 82.9(2).



halide ArX to a Ni(0) complex and disproportionation^{5e,10b} of [Ni(Ar)(X)(bpy)] (cf. Experimental section).

The use of usual ArX (e.g., phenyl halides and tolyl halides) or moderately electron-withdrawing ArX such as NC(C₆H₄)Cl-*p* in the reaction with Ni(0) complexes did not give the [NiAr₂(bpy)]-type complex. In these cases, the reaction gave the coupling product Ar-Ar^{5e,12f} or stopped at the oxidative addition to yield [Ni(Ar)(X)(bpy)].^{12d,f,13} [NiAr₂(bpy)] was isolable only for highly electron-withdrawing Ar groups as in **2a–2c**.

It was reported that *cis*-[Ni(Me)(Ar)(dpe)]^{2h} (dpe = 1,2-bis(diphenylphosphino)ethane) underwent reductive elimination much more easily than *cis*-[NiMe₂(dpe)], and attempts to prepare *cis*-[NiAr₂(bpy)] with non-electron-withdrawing Ar groups were unsuccessful. These results suggest a strong inclination of *cis*-[NiAr₂(bpy)] to undergo the reductive elimination. The ease of the reductive elimination of Ar-Ar from [NiAr₂(bpy)] may be related to the presence of the π-orbital at the Ni-C carbon. For example, the π-orbitals on C₁ and C₇ carbons of **2a** (Fig. 1) seem to overlap each other and such overlapping may enhance the reductive elimination of Ar-Ar from [NiAr₂(bpy)].

When the Ar group is highly electron-withdrawing, the *cis*-[NiAr₂(bpy)]-type complexes are isolable, as exemplified by **2a–2c**. The Ni–Ar bond is considered to be polarized as Ni^{δ+}-Ar^{δ-} and the reductive elimination of electrically neutral Ar-Ar will require a partial shift of electrons from the Ar group to Ni;¹⁴ this explains the higher stability of [NiAr₂(bpy)] with the more strongly electron-withdrawing Ar group.¹⁴

UV-Vis Data for Electronic State of [NiAr₂(bpy)]. Figure 2 compares the UV-vis spectra of **1b**, **2b**, and **2c**. UV-vis data of **1a–1c** have already been reported previously.^{2a}

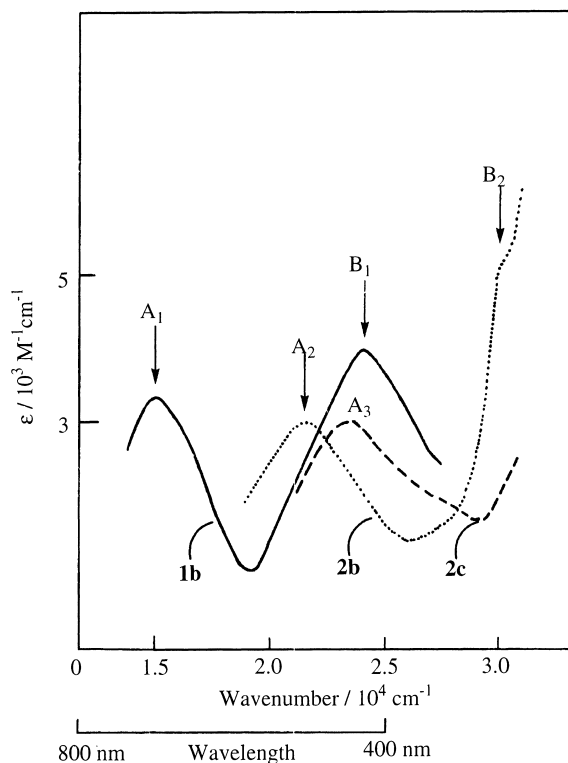


Fig. 2. UV-vis spectra of **1b** (—), **2b** (·····), and **2c** (---) in THF. For A₁, A₂, A₃, B₁, and B₂, see Fig. 3. The shoulder peak of **2b** at about 29000 cm⁻¹ becomes clearer in DMSO.

Low valent Ni-bpy complexes such as **1b** usually give rise to two MLCT (Ni → bpy) bands, e.g., A₁ and B₁, as shown in Figs. 2 and 3 with a molar absorption coefficient (ϵ) of $3\text{--}4 \times 10^3 \text{ M}^{-1} \text{ cm}^{-1}$. The A₁ and B₁ arrows in Fig. 3 represent assignments of the two MLCT bands of **1b**, which has been confirmed from UV-vis data measured under various conditions.^{2a}

2b shows an A₂ peak at 21600 cm⁻¹ (462 nm; cf. Fig. 2) in THF, which is assigned to an Ni → π_1^* MLCT transition as indicated by arrow A₂ in Fig. 3. **2b** shows a B₂ shoulder peak at about 29000 cm⁻¹, and this absorption peak seems assignable to another Ni → π_2^* MLCT transition (B₂ in Fig. 3). The energy difference (29000–21600 = 7400 cm⁻¹) between the A₂ and B₂ transitions roughly agrees with that (7300 cm⁻¹) between π_1^* and π_2^* levels of bpy¹⁵ depicted in Fig. 3, supporting the assignment. **2c** gives an absorption peak A₃; however, in this case, the corresponding B₃ peak seems to be hidden under a strong $\pi\text{--}\pi^*$ transition band of bpy.

Based on the assumption that the A and B peaks of complexes **2a–2c** can also be assigned to the MLCT transition, the energy level of the highest energy orbital (occupied d orbital) at Ni can be evaluated, as shown in Fig. 3. Due to the electron-withdrawing nature of the Ar group, the energy of the orbital at Ni of [NiAr₂(bpy)] is lowered compared with that of [NiR₂(bpy)].

In view of the energy level of the d-orbital of Ni, the electron-withdrawing ability of the Ar group is considered to increase in the order: C₃N₂(CH₃)₂Cl (in **2b**) < C₃N₂(CH₃)-(COOCH₃)Cl (in **2c**) < C₆F₅ (in **2a**). Energy levels of σ and σ^* orbitals of HCl evaluated from the ionization potential and

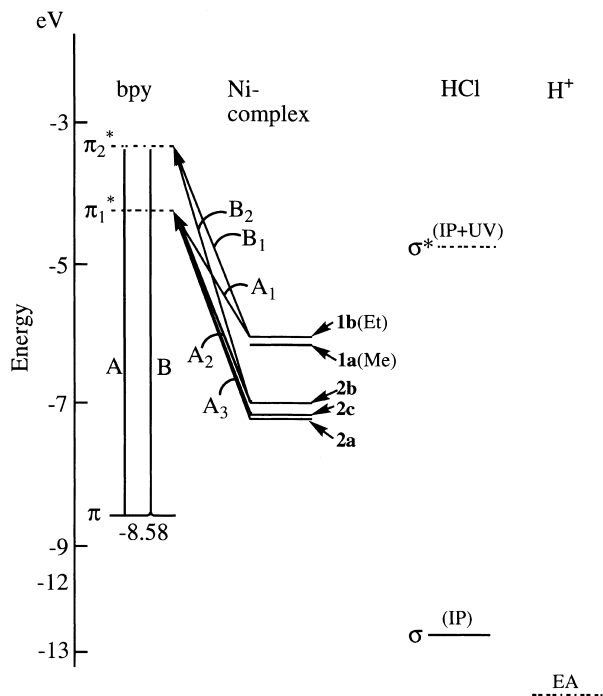
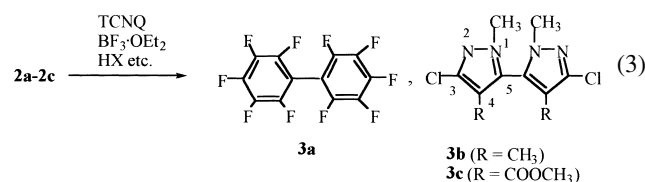


Fig. 3. Energy diagram of bpy, Ni complexes, and HCl. π (HOMO) level of bpy is estimated from its IP.¹⁵ σ and σ^* levels of HCl are estimated from its IP^{16a} and UV absorption peak.^{16b} The 1s energy of H is shown for the electron affinity of H⁺.

the absorption peak, as well as electron affinity of H⁺,¹⁶ are also illustrated in Fig. 3, the discussion of which will be given later.

The A₂ peak of **2b** and the A₃ peak of **2c** shift depending on the kind of solvent in which the complex is dissolved. As shown in Fig. 4, plots of the energy of the absorption peaks A₂ and A₃ (Fig. 2) vs Kosower's Z values¹⁷ give a linear positive correlation, supporting the assumption that the absorption band is assignable to a kind of CT band.

The stable complexes **2a–2c**, however, undergo reductive elimination when they interact with strong π -acids (e.g., TCNQ), Lewis acids, and Brønsted acids (data shown in runs 18–25 in Table 1 and data in Table 2).



The characterization of **3a–3c** is given in the experimental part. The molecular structure of **3c** as determined by X-ray crystallography is shown in the supporting data. In contrast to the reaction of **2a–2c** with Brønsted acid, reactions of **1a** and **1b** with Brønsted acids normally evolved RH, methane and ethane, respectively. The reductive elimination of **1a–1c** caused by the electron-accepting aromatic compounds and that of **2a–2c** caused by Brønsted acids have been studied kinetically and spectroscopically, and the obtained results are discussed in the following part.

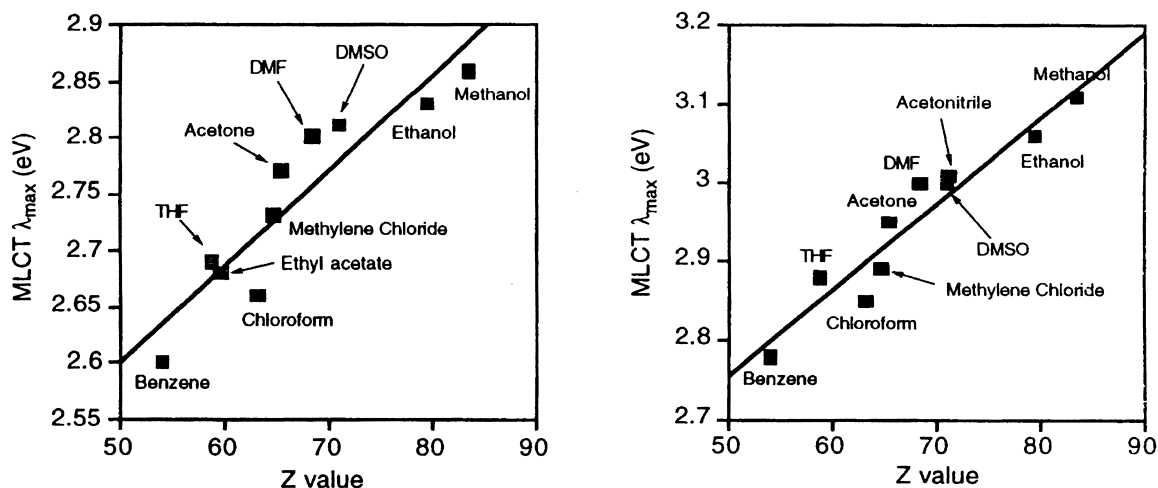


Fig. 4. Plots of the energy of the A₂ peak of **2b** (left) and A₃ peak of **2c** (right) vs Kosower's Z value.¹⁷

Reductive Elimination of 1a-1c Caused by Electron-Accepting Aromatic Compounds. [NiR₂(bpy)] is stable in solvents commonly used for UV-vis spectroscopy at room temperature under N₂. However, as described above, the reaction of **1a-1c** with electron-accepting aromatic compounds causes reductive elimination with the liberation of R-R and changes in the UV-vis spectrum.

When the aromatic compound has an Ar-CN or Ar-F bond, prolonged reaction leads to oxidative addition of the Ar-CN¹⁸ or Ar-F bond to [Ni(bpy)]. This nickel(0) complex is considered to be formed according to the reductive elimination and to be stabilized by coordination of solvent, however, it undergoes the reaction with the Ar-CN and Ar-F compounds to yield the corresponding oxidative addition products (e.g., [Ni(CN)(C₆H₄CN-*p*)(bpy)]).

Figure 5 shows changes of the UV-vis spectrum during the reactions of **1b** and **1c** with C₆H₄(CF₃)₂-*p*, and C₆F₆, respectively. The reaction proceeds with isosbestic points. Other combinations of **1a-1c** and electron accepting-aromatic compounds give analogous spectroscopic changes.¹⁹ Kinetic and spectroscopic studies of the reaction reveal the following features of the reaction.

(i) The plot of log (Abs(*t*) - Abs(∞)) (Abs(*t*) = absorbance at peak A (e.g., A₁ for **1b**) at time *t*; Abs(∞) = absorbance at peak A at infinite time) shown in Figure 5 against time *t* gives a straight line, indicating that the reaction follows the first-order kinetics with respect to concentration of [NiR₂(bpy)]. The slope of the straight line increases linearly with the concentration of the electron-accepting aromatic compound, affording the following rate equation.

$$-d[\mathbf{1}]/dt = k[\mathbf{1}][\text{electron-accepting aromatic compound}] \quad (4)$$

(ii) As shown in Fig. 6, plots of the logarithm of the second-order rate constant *k* obtained for **1b** vs the sum of the Hammett σ_p values of the substituents, $\Sigma\sigma_p$, in the electron-accepting aromatic compound reveals a trend that the accelerating effect on the reductive elimination increases with an increase in the electron-accepting ability of the aromatic compound. Except for C₆H₅NO₂, a roughly linear correlation holds between *k*

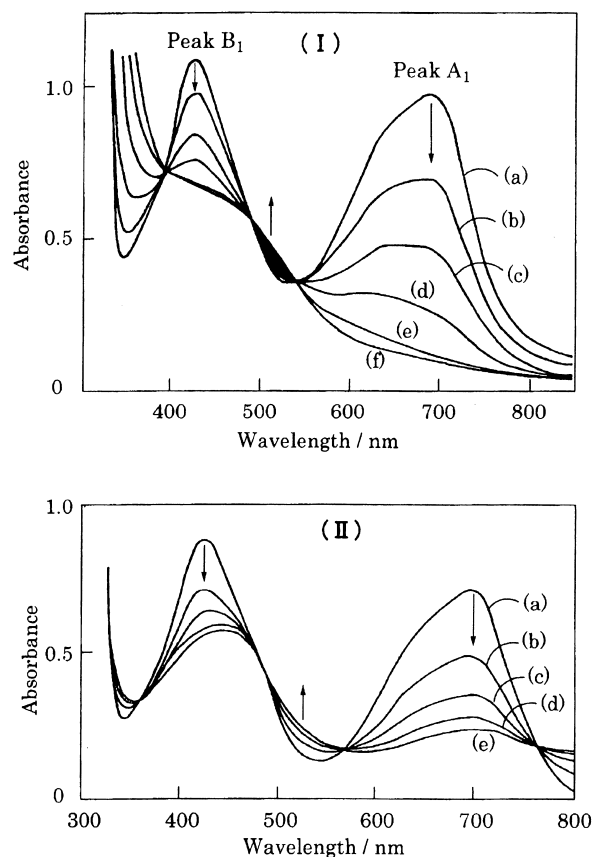


Fig. 5. Upper graph (I): reaction of [NiEt₂(bpy)] **1b** with C₆H₄(CF₃)₂-*p* (2.2 M) at 25 °C in THF. Time/10² s: (a) 0; (b) 350; (c) 760; (d) 1500; (e) 3200; (f) ∞. Lower graph (II): reaction of NiPr₂(bpy) **1c** with C₆F₆ (0.091 M) at 34.5 °C in THF. Time/10² s: (a) 0; (b) 12; (c) 24; (d) 36; (e) ∞.

and $\Sigma\sigma_p$ with a slope of about 1.8.

C₆H₅NO₂ exceptionally strongly accelerates the reductive elimination. This may be due to the direct attack of the positively charged C^{δ+}-NO₂^{δ-} carbon center at the nucleophilic Ni in **1b** rather than the electrophilic attack of the aromatic compound through the benzene ring.

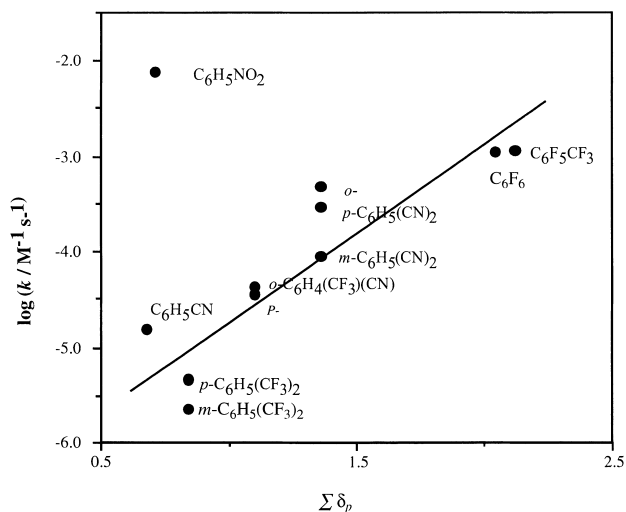
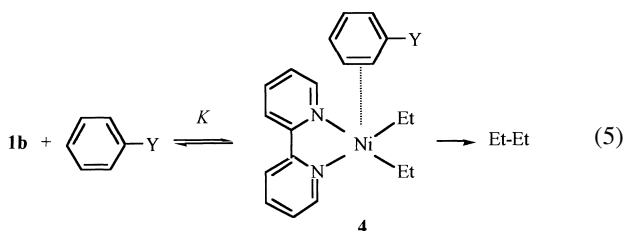


Fig. 6. Plot of $\log k$ obtained with **1b** at 25 °C vs $\Sigma\delta_p$ of the electron-accepting aromatic compound. In THF.

(iii) As shown in Fig. 6, the k values observed for **1b** at 25 °C are in a range of about 10^{-5} – 10^{-2} $\text{M}^{-1} \text{s}^{-1}$. These k values are considerably smaller than those ($k = 10^{-4}$ – 10^{-1} $\text{M}^{-1} \text{s}^{-1}$) observed for the similar reductive elimination of **1b** caused by electron-accepting olefins.^{2a} The Eyring plot of the k value gives a straight line. The kinetic parameters (ΔG^\ddagger , ΔH^\ddagger , ΔS^\ddagger) estimated from the slope and intercept of the line are listed in the supporting data.

(iv) The k value increases in the order of **1a** < **1b** < **1c**. Plots of $\log k$ values obtained in reactions with $\text{C}_6\text{F}_5\text{CF}_3$ vs Taft's σ^* value²⁰ of the R group in **1a**–**1c** give a straight line with a slope of -0.72 . For the acceleration of the reductive elimination of **1a**–**1c** caused by an electron-accepting olefin (methyl acrylate), similar plots gave a straight line with a slope of -2.5 .^{2a}

The reductive elimination caused by the aromatic compound seems to take place through the π -coordination of the aromatic compound with Ni of $[\text{NiR}_2(\text{bpy})]$.



Variable temperature ¹H-NMR spectroscopy indicates that the position of the CH₃ signal shifts slightly as the temperature is lowered.^{9d} In contrast, the peak position of the CH₂ signal shifts in the direction of the upper magnetic field.^{9d} This shift of the CH₂ peak is reasonably accounted for by an anisotropic up-field magnetic effect²¹ of the coordinated aromatic ring in **4** and a shift of the equilibrium (K in Eq. 5) in the direction of **4** at low temperature. On the other hand, the CH₃ group will receive the magnetic effect to a lesser extent. π -Arene complexes of Ni have been reported.^{22,23}

All these results are consistent with the enhancement of the reductive elimination by coordination of the electron-accepting aromatic compound.

The enhancement effect of the electron-accepting olefin and the aromatic compounds may be associated with the results of synthetic C–C coupling reactions promoted by Ni, if the reductive elimination step is a rate determining step. For example, the coupling reaction between RMgX and $\text{R}'\text{X}$, $\text{RMgX} + \text{R}'\text{X} \rightarrow \text{R-R}'$, has been successfully carried out when *olefinic halide* or *aryl halide* is used as $\text{R}'\text{X}$, whereas the coupling reaction does not proceed well by using alkyl halides.^{5b} In contrast, there is no restriction on the kind of R group in RMgX , suggesting that enhancement of the reductive elimination of $\text{R-R}'$ from a supposed intermediate species $[\text{Ni}(\text{R})(\text{R}')\text{L}_n]$ by coordination of the electron-accepting *olefinic halide* or *aryl halide* is essential for the catalytic reaction. For some other metal-promoted synthetic reactions, however, such a difference between olefinic or aryl halide and aliphatic halide may not be important. Facile reductive elimination reaction of Ni-sp²-C compound discussed above is also considered. Ni-catalyzed coupling reactions are promoted in the presence of dienes,^{7f} and it has recently been reported that Ni-catalyzed cross coupling of Grignard reagent proceeds with alkyl halides in the presence of dienes^{5f} which will cause back-donation from nickel. Effects of electron-accepting olefin to promote Ni-catalyzed coupling reactions were also reported.^{2e–g} The reductive elimination of Et–Et from **1b** in the presence of phenyl chloride was previously reported.^{2c}

Reductive Elimination Promoted by Brønsted Acid.

Organotransition metal complexes $[\text{MYL}_n]$ usually undergo protonolysis in the reaction with Brønsted acid to produce YH .^{1,10}



However, for the isolated $[\text{NiAr}_2(\text{bpy})]$ with the electron-withdrawing Ar group used in this study, the reaction of $[\text{NiAr}_2(\text{bpy})]$ with Brønsted acids HX leads to reductive elimination to produce Ar–Ar.



2a–**2c** were stable at 150 °C even in air, and thermolyses of **2b** and **2c** started at 178 °C and 306 °C under N₂, respectively. **2a**, **2b**, and **2c** were stable in DMF and DMSO solution at 60 °C for 5 h. However, such stable nickel complexes undergo reductive elimination in the presence of a Brønsted acid. For example, the reactions of **2b** and **2c** with hydrochloric acid (6 M) and nitric acid (6 M) in air gave **3b** and **3c** in 55 and 97% isolated yields, respectively.

Table 2 summarizes the results of the reactions of $[\text{NiAr}_2(\text{bpy})]$ with HX . As shown in Table 2, the ratio of the two products, Ar–Ar and ArH, depends on the kind of HX and the atmosphere to which the reaction is exposed. The data given in Table 2 and other experimental results reveal the following features of the reductive elimination promoted by the Brønsted acid.

(i) Addition of CF_3COOH to a solution of **2a** in air leads to quantitative reductive elimination (run 1 in Table 2). Figure 7 shows changes in the ¹⁹F-NMR spectrum on addition of CF_3COOH to a DMSO-*d*₆ solution of **2a**. The ¹⁹F-NMR data reveal that $\text{C}_6\text{F}_5\text{-C}_6\text{F}_5$ is the sole product in the reaction of **2a**

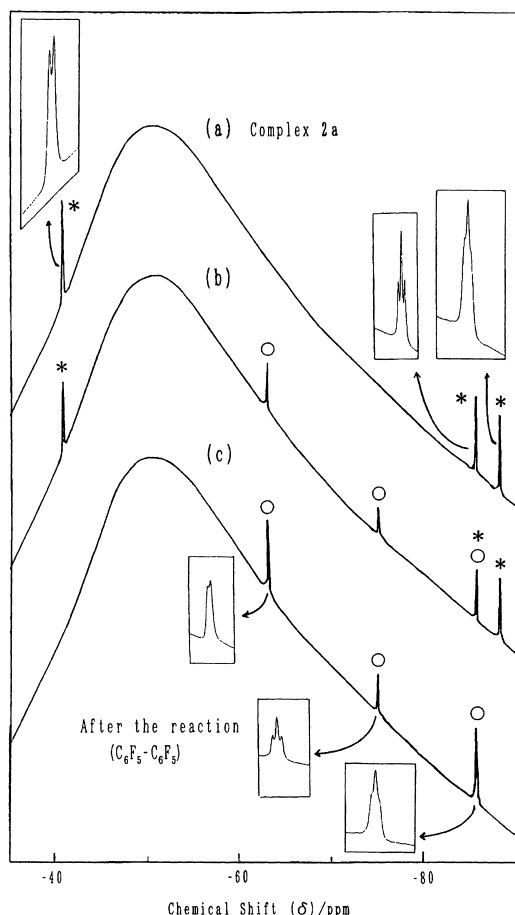
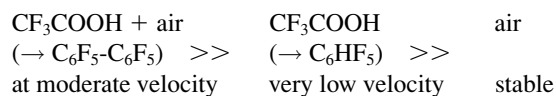


Fig. 7. Changes in the ^{19}F -NMR spectrum of **2a** on addition of CF_3COOH (2.3 M) to a $\text{DMSO}-d_6$ solution of **2a** in air. (a): before addition of CF_3COOH ; (b) 5 h after addition of CF_3COOH (2.3 M) at 40°C ; (c) after completion of the reaction. The chemical shift δ is referred to CF_3COOH . The signals marked by an asterisk (*) are due to **2a**, whereas those marked by an open circle (O) are due to $\text{C}_6\text{F}_5\text{-C}_6\text{F}_5$. The strong and broad peak centered at about $\delta = -50$ ppm is due to Teflon in the NMR instrument.

with CF_3COOH . In the case of the reaction of **2a** with CF_3COOH , in the absence of O_2 or air, the hydrolysis of **2a** by CF_3COOH to give C_6HF_5 (run 2 in Table 2) proceeds very slowly. Type and velocity of reactions of **2a** with CF_3COOH and air:



HCOOH also promotes the reductive elimination in air, as proved by ^{19}F -NMR spectroscopy but at a considerably lower reaction rate than CF_3COOH . The importance of O_2 in the reductive elimination is also observed in the reaction of **2a** (run 4) and **2b** with HCl (runs 6–8). **2b** shows considerable stability in an aqueous solution of 0.3 M HCl under N_2 at room temperature. On raising the temperature to 50°C under N_2 , protonolysis of **2b** takes place (run 8). However, in the presence of

air or O_2 , both protonolysis and reductive elimination are promoted, and in pure O_2 the reductive elimination becomes predominant (run 7).

Brønsted acids may promote the reductive elimination by interacting with the Ni center or the nitrogen in the bpy ligand. However, the latter case seems unlikely since (a) the acceleration effect of acid varies depending on the kind of acid as described later, (b) the effect of O_2 is difficult to explain on the basis of the interaction with the nitrogen of bpy, and (c) $[\text{NiCl}_2(\text{bpy})]$ is isolated in about 50% yield after the reductive elimination in the presence of HCl .

Acceleration of the reductive elimination by interaction of the Brønsted acid with nitrogen in the pyrazolyl ligand of **2b** is less likely. There are two reasons: (a) the reductive elimination products, bipyrazoles **3b** and **3c** (cf. Eq. 3), are not protonated with diluted acids presumably due to the weak basicity of **3b** and **3c**; and (b) **2a** with the C_6F_5 ligand also undergoes the reductive elimination promoted by the Brønsted acid.

(ii) HBr promotes the reductive elimination reaction of **2a** and **2b** both in the presence and in the absence of O_2 (runs 5, 9, and 10). The specific effect of HBr may be related to its unique redox behavior.²⁴ For the HBr -promoted reductive elimination, the evolution of H_2 was confirmed by gas chromatography. In the case of the HCl -promoted reductive elimination in air, H_2 was not detected and the consumption of O_2 was observed instead.

In order to obtain further information regarding the reductive elimination, the following spectroscopic and kinetic studies on the reaction of Brønsted acids with **2a** and **2b** have been carried out. Although further research seems to be necessitated to clarify detailed reaction mechanism, the following data reveal several features of the reductive elimination.

Spectroscopic Data and Equilibrium. Since the reductive elimination caused by the Brønsted acid does not proceed rapidly, the interaction of the Brønsted acid with $[\text{NiAr}_2(\text{bpy})]$ can be investigated by UV-vis spectroscopy.

Figure 8 shows changes in the UV-vis spectrum of **2b** on addition of H_2SO_4 . As indicated in Fig. 8, the spectrum changes with clear isosbestic points at 315, 335, 345, and 418 nm, suggesting that there exists the following simple equilibrium:



If such an equilibrium is assumed, the equilibrium constant K_a is given by the following Eq. 8:

$$K_a = \frac{[\mathbf{5}]}{[\mathbf{2b}][\text{HX}]} = \frac{(x-y)}{(y-y_\infty)[\text{HX}]}, \quad (8)$$

where x is the absorbance of the initial solution containing **2b** at 450 nm, and y represents the absorbance after the addition of the Brønsted acid, as shown in Fig. 8; y is assumed to become y_∞ when the completely shifted to the right. From Eq. 8, Eq. 9 is derived

$$\frac{(x-y)}{y[\text{HX}]} = K_a - \frac{(y_\infty K_a)}{y}, \quad (9)$$

and Fig. 9 exhibits plots of the $(x-y)/y[\text{HX}]$ value vs $1/y$ for the data shown in Fig. 8.

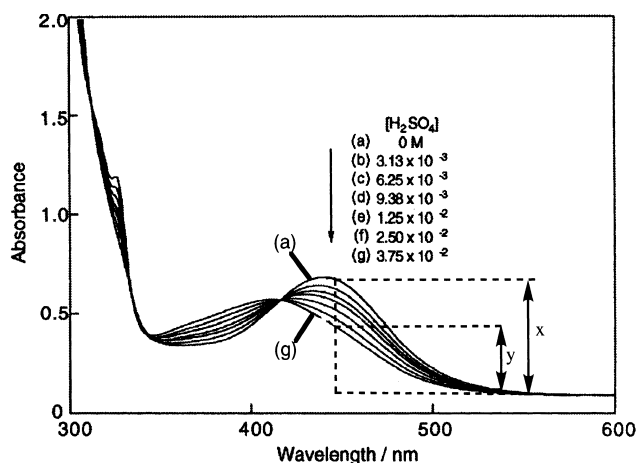


Fig. 8. Changes of the UV-vis spectrum of **2b** on addition of H₂SO₄ at 300.5 K under air. In DMSO. [**2b**] = 1.4 × 10⁻³ M. [H₂SO₄]/10⁻³ M: (a) 0, (b) 3.13, (c) 6.25, (d) 9.38, (e) 12.5, (f) 25.0, and (g) 37.5.

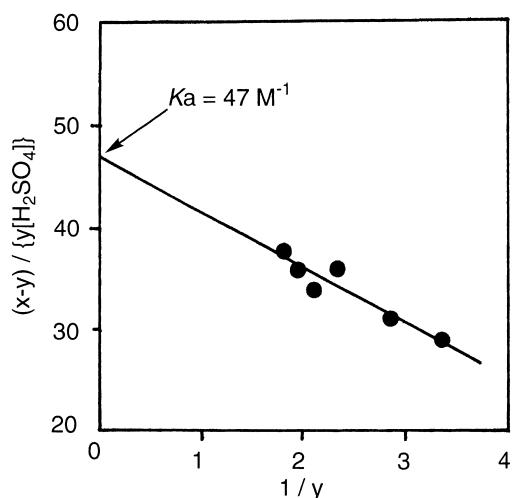


Fig. 9. Plots of the $(x-y)/[y[H_2SO_4]]$ value vs the $1/y$ value for the UV-vis spectra shown in Fig. 9. In DMSO.

From the intercept and the slope of the straight line in Fig. 9, K_a and y_∞ are evaluated as 47 M⁻¹ and 0.12, respectively. Table 3 summarizes K_a values obtained with the Brønsted acids. The van't Hoff plot of the K_a value obtained with H₂SO₄ vs $1/T$ gives ΔH° and ΔS° values of -10.1 kJ mol⁻¹ and -2.4 J K⁻¹

Table 3. K_a Values for the Formation of the Adduct between **2b** and Protic Acids

No.	Protic acids	Temp/K	K_a/M^{-1}	
1	H ₂ SO ₄	N ₂	300.0	43.7
2	H ₂ SO ₄	N ₂	306.0	39.5
3	H ₂ SO ₄	N ₂	308.0	37.3
4	H ₂ SO ₄	N ₂	316.5	35.4
5	H ₂ SO ₄	Air	300.5	46.5
6	HCl	N ₂	313.0	38.4
7	HBr	N ₂	301.2	21.6
8	HNO ₃	Air	300.5	41.0

mol⁻¹, respectively. Tolman reported²⁵ a similar equilibrium for the formation of an adduct between [Ni[P(OEt₃)₄]] and H₂SO₄ in CH₃OH and formulated the equilibrium as



For the proposed equilibrium, Tolman obtained a K_1 value of 33 M⁻¹, which is comparable to the K_a values summarized in Table 3.

The equilibrium for the present system may also be formulated (instead of Eq. 7) as:



However, we favor Eq. 7, since X in HX affects the conditions of the reductive elimination, as will be described later, and the dissociation constant of HX in organic solvents is small.²⁶

According to the adduct formation with Brønsted acid (or H⁺), the A₂ absorption peak of **2b** (cf. Figs. 2, 3, 4, and 8) at 440 nm in DMSO shifts by about 25 nm (or by 0.17 eV) to the shorter wavelength region, as shown in Fig. 8. This shift is reasonably explained by the lowering of the d orbital energy due to the coordination of **2b** with the Brønsted acid (or H⁺), which will cause partial electron migration from Ni to the σ^* orbital of HX (cf. Fig. 3). Other Brønsted acids also lead to similar shifts of the A₂ peak of **2b** to the shorter wavelength region. However, the addition of H₂SO₄ to a DMSO solution of **2a** did not cause such an obvious shift of the UV-vis peak, revealing that **2a** had only a weak interaction with H₂SO₄ due to the lower d orbital of **2a** (Fig. 3), which would bring about less extensive electron migration from Ni to the σ^* orbital of the acid (or to H⁺).

Kinetics of the Reductive Elimination. Some reactions with Brønsted acids have been analyzed kinetically.

2a-CF₃COOH. The UV-vis spectrum of **2a** in tetrahydrofuran (THF) in air did not show any observable change with time. However, when CF₃COOH was added to the THF solution, the UV-vis spectrum showed a decrease of **2a** with time, in accordance with the ¹⁹F NMR data shown in Fig. 7. The decay curve of **2a** obeys the pseudo first-order rate law, and the pseudo-first-order rate constant increases linearly with [CF₃COOH], resulting in the following rate equation:

$$d[2a]/dt = k'[2a][CF_3COOH] \quad (12)$$

The k' value at 40 °C is 3.2 × 10⁻⁵ M⁻¹ s⁻¹.

2b-H₂SO₄. Figure 10 exhibits changes in the UV-vis spectrum during the reaction of **2b** with H₂SO₄ in DMSO under air. Kinetic results obtained from the UV-vis spectrum indicate that the reaction obeys the second-order rate law with respect to [**2b**]. The pseudo second-order rate constant increases linearly with O₂ pressure in the atmosphere with which [O₂] in the solution is equilibrated:

$$-d[2b]/dt = k''[2b]^2[O_2] \quad (13)$$

The third-order rate constant k'' is evaluated as 2.2 M⁻² s⁻¹ at 306 K by using the Henry coefficient of 12 mM bar⁻¹ for usual organic solvents.²⁷

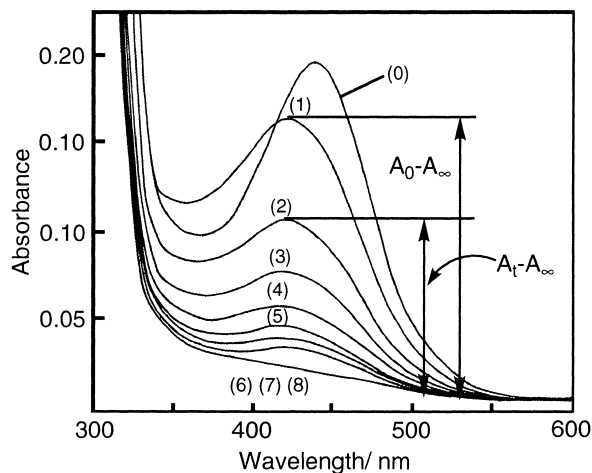


Fig. 10. Changes in the UV-vis spectrum during the reaction of **2b** (4.7×10^{-5} M) with H_2SO_4 (1.2×10^{-2} M) in DMSO at 300 K under air. Reaction time: (1) 0 h; (2) 2 h; (3) 4 h; (4) 6 h; (5) 8 h; (6) 10 h; (7) 12 h; (8) ∞ . Curve (0) represents the UV-vis spectrum of **2b** before addition of H_2SO_4 (cf. Fig. 8).

Under O_2 , the k'' value varies with $[\text{H}_2\text{SO}_4]$, as depicted in Fig. 11. The saturating trend at high $[\text{H}_2\text{SO}_4]$ (or Michaelis–Menten type profile) may be a reflection of the adduct creating equilibrium between **2b** and H_2SO_4 as discussed above (Eqs. 7–11).

These kinetic results indicate that the activation of Ni–C bonds in **2b** takes place by coordination of both H_2SO_4 and O_2 and suggest the formation of a 2:2:1 adduct of **2b**, H_2SO_4 , and O_2 such as that shown in Scheme 2. Water is considered to be formed in the reaction.

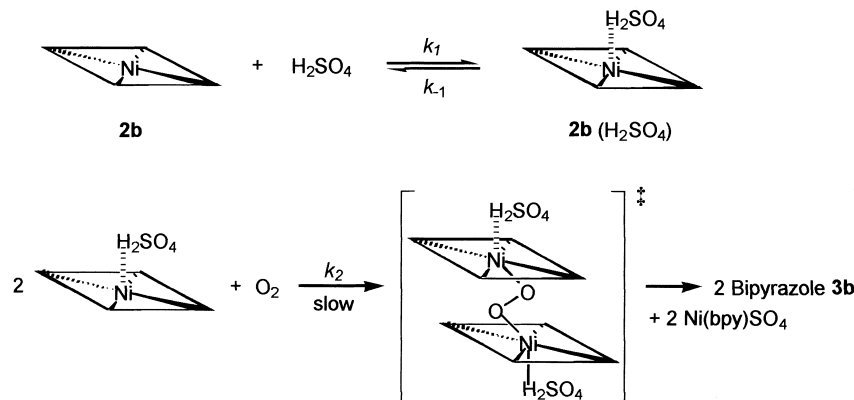
Such μ -peroxo complexes of transition metals are known.²⁸

2b-HBr. As described above, this reaction proceeds even under N_2 to liberate **3b**. Following the reaction by UV-visible spectroscopy under N_2 gave the following kinetic results.

(i) Plots of $[\mathbf{2b}]^{1/2}$ against time t give a straight line, revealing that the reaction obeys the following rate equation:

$$-d[\mathbf{2b}]/dt = k_{\text{obs}} [\mathbf{2b}]^{1/2} \quad (14)$$

(ii) Plots of $\ln k_{\text{obs}}$ vs $\ln [\text{HBr}]$ gives a straight line with a slope of about 4, as depicted in Fig. 12.



Scheme 2.

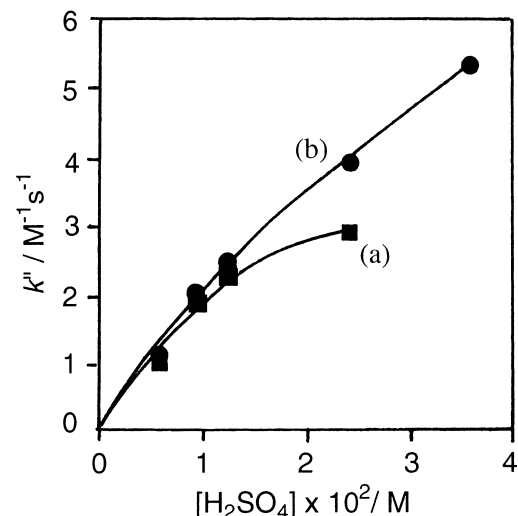
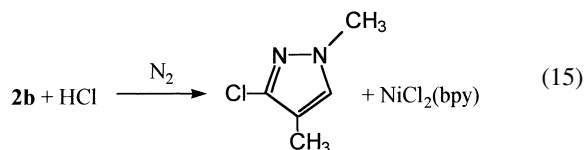


Fig. 11. Dependence of the initial concentration of H_2SO_4 on the pseudo-second-order rate constant k'' for the reaction of complex **2b** with H_2SO_4 under O_2 at (a) 33.0 °C and (b) 43.0 °C. In DMSO.

Although the details are not yet clear, the reductive elimination of **3b** from **2b** caused by the interaction with HBr is considered to proceed via electron transfer assisted by several HBr molecules.

2b-HCl under N_2 . As described above, this reaction gives the hydrolysis product of **2b**, 3-chloro-1,4-dimethylpyrazole (Eq. 15). Kinetic study on this reaction by UV-vis spectroscopy reveals the following features of the reaction.



(i) The reaction obeys the pseudo first-order rate law with respect to **2b**, and the pseudo first-order rate constant linearly increases with $[\text{HCl}]$ to give the second-order rate equation:

$$R = k''' [\mathbf{2b}][\text{HCl}] \quad (16)$$

where the k''' value at 313.0 K is $4.3 \times 10^{-3} \text{ M}^{-1} \text{ s}^{-1}$.

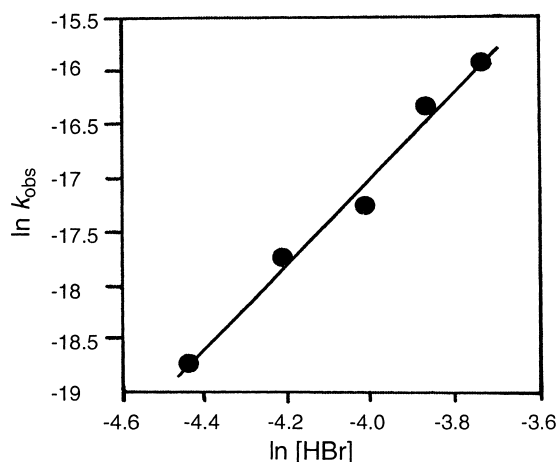
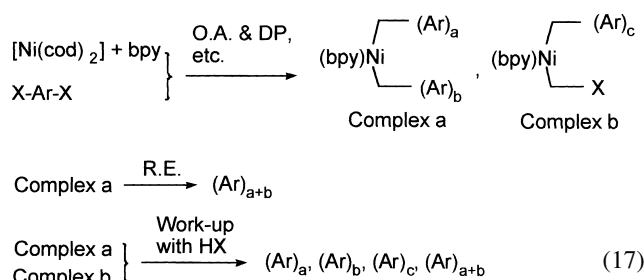


Fig. 12. Dependence of k_{obs} (in $\text{M}^{1/2} \text{s}^{-1}$) on the initial concentration of KBr (in M) for the reaction of **2b** with HBr under N_2 . In DMSO.

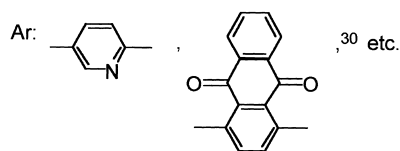
(ii) Temperature dependence of the k''' value gives the following kinetic parameters at 313 K: $E_a = 105 \text{ kJ mol}^{-1}$; $\Delta H^\ddagger = 103 \text{ kJ mol}^{-1}$; $\Delta S^\ddagger = 37 \text{ J mol}^{-1} \text{ K}^{-1}$; $\Delta G = 91 \text{ kJ mol}^{-1}$.

(iii) Use of DCl affords an isotope effect, $k'''(\text{HCl})/k'''(\text{DCl})$, of 2.8, which is within the a range of values for the primary isotope effect, suggesting that direct interaction of H of HCl (or H^+) with the Ni center takes place in the reaction.

Effects on Polymer Synthesis. Various electron-accepting π -conjugated polymers have been prepared according to the Ni(0)-complex (typically a mixture of $[\text{Ni}(\text{cod})_2]$ and bpy) promoted dehalogenation polycondensation^{7f} of dihaloaromatic compounds; such polymerization is considered to proceed via the reductive elimination from an $[\text{Ni}(\text{aryl})_2(\text{bpy})]$ -type propagating species (Eq. 17).²⁹ Polypyridine²⁹ and polyanthraquinone³⁰ are typical electron-accepting π -conjugated polymers and behave as n-type conducting materials when one constructs electronic devices.³¹ The $(\text{Ar})_a$, $(\text{Ar})_b$ and $(\text{Ar})_c$ groups in complexes a and b may be combined with other Ni species, since the obtained polymers^{29,30} did not contain halogen and were H-terminated.



O.A. = oxidative addition, DP = disproportionation
R.E. = reductive elimination



After the polymerization, the reaction mixture is usually treated with aqueous HCl. However, in view of the present re-

sults described above, treatment of the reaction mixture with H_2SO_4 and CF_3COOH in air will give a polymer with a higher molecular weight; the Complex a is considered to give $(\text{Ar})_{a+b}$, $(\text{Ar})_a$, and $(\text{Ar})_b$ in the work-up with HX, and treatment with H_2SO_4 and CF_3COOH will increase the proportion of $(\text{Ar})_{a+b}$. We have divided the reaction mixture obtained from $[\text{Ni}(\text{cod})_2]$, bpy, and 2,5-dibromo-6-hexylpyridine into two portions, treated the two portions with HCl under N_2 and H_2SO_4 in air, respectively, and compared the molecular weights of the polymers. The polymerization was carried out with 1.5 mol of $[\text{Ni}(\text{cod})_2]$ per 1 mol of 2,5-dibromo-6-hexylpyridine; the yield of the polymer was 80% (Scheme 3).

GPC analysis reveals that the number average molecular weight, M_n , and weight average molecular weight, M_w , increase in the order of **polymer-1** ($M_n = 2100$; $M_w = 3600$) < **polymer-2** ($M_n = 6400$; $M_w = 31000$), as expected from the above described results. Gel permeation chromatograms of the polymers are exhibited in Fig. 13. The use of HBr, HCl, CF_3COOH in a similar polymerization of 2,5-dibromopyridine, however, did not cause a significant difference in the molecular weight of the obtained polymer, indicating that such effect of the acid depends on the polymerization system.

Conclusion

The reductive elimination of R-R from $[\text{NiR}_2(\text{bpy})]$ is promoted by coordination with electron-accepting aromatic compounds, whereas the reductive elimination of Ar-Ar from $[\text{NiAr}_2(\text{bpy})]$ is caused by interaction with Brønsted acids. For the latter reductive elimination, an assisting effect of O_2 has been revealed. These results support the view that interaction with electron-accepting molecules, in general, activates the Ni-C bonds in diorgano(2,2'-bipyridyl)nickel(II) complexes. The obtained information contributes to a better understanding of Ni-promoted synthetic reactions.

Experimental

Materials. Electron-withdrawing aromatic compounds, Lewis acids, Brønsted acids, C_6F_5 - C_6F_5 , and C_6HF_5 were used as purchased. $[\text{Ni}(\text{cod})_2]$,³² **1a-1c**,^{2a} and **2b-2c**^{9c} were prepared as previously reported. **2a** was prepared from $[\text{Ni}(\text{cod})_2]$ (2.4 g, 8.7 mmol), cod (0.6 mL), bpy (1.4 g, 8.7 mmol), and C_6F_6 (4.3 g, 23 mmol) in THF (50 mL). After 24 h at room temperature, hexane was added to the reaction mixture to obtain a precipitate. Work-up, including extraction of $[\text{Ni}(\text{C}_6\text{F}_5)_2(\text{bpy})]$ with toluene, gave 2.2 g (4.0 mmol) of $[\text{Ni}(\text{C}_6\text{F}_5)_2(\text{bpy})]$. ^1H NMR(DMSO- d_6): δ 8.54 (d, 2H), 8.25 (t, 2H), 7.54 (t, 2H), 7.47 (d, 2H). ^{19}F NMR(DMSO- d_6) ppm from external CF_3COOH : -38.56 (d, $J = 28\text{Hz}$), 82.83 (t, $J = 21\text{Hz}$), 85.47 (t, $J = 20\text{Hz}$ or dd). The IR spectrum agreed with that of **2a** prepared via a different route.^{9d} The crystal for X-ray crystallography was obtained by recrystallization from acetone at -20°C and was formulated as $[\text{Ni}(\text{C}_6\text{F}_5)_2(\text{bpy})(\text{acetone})]$. In Fig. 1, acetone is omitted for simplification.

3b was prepared by treating a chloroform (20 mL) solution of **2b** (30 mg) with an aqueous solution of HNO_3 (6 M, 10 mL). Purification by column chromatography (SiO_2 , $\text{CH}_3\text{COOC}_2\text{H}_5$) gave a white powder of **3b** in 57% yield. Mp $87\text{--}88^\circ\text{C}$. ^1H NMR(DMSO- d_6) δ 1.83 (s, 6H, CH_3), 3.59 (s, 6H, CH_3). HRMS: Found: m/z 258.0367; Calcd for $\text{C}_{10}\text{H}_{12}\text{Cl}_2\text{N}_4$: $M = 258.0439$. **3c** was prepared analogously in 97% yield. ^1H NMR(CDCl_3) δ 3.65 (s, 6H, CH_3), 3.72 (s, 6H, CH_3). HRMS: Found 346.0175; Calcd

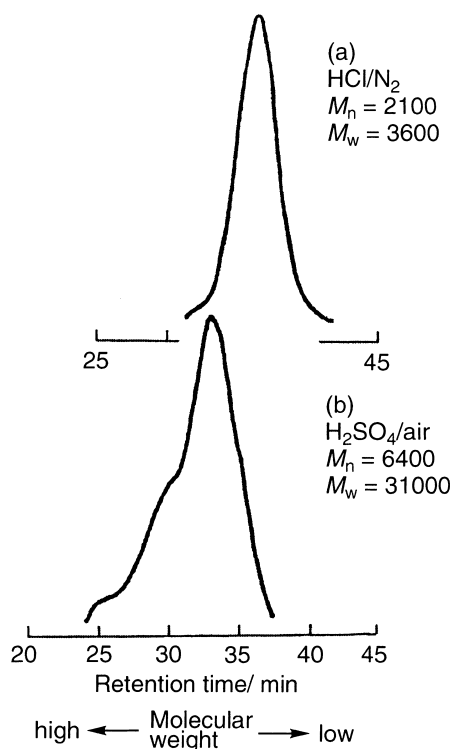
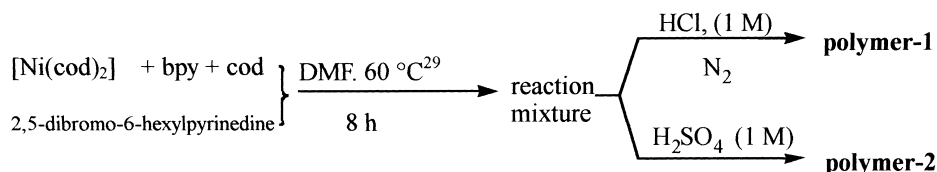


Fig. 13. Gel permeation chromatograms of poly(6-hexylpyridine), P6HexPy, (vs polystyrene standards). For (a) P6HexPy obtained after treatment of the polymerization mixture with HCl (1 M) under N₂ (**polymer-1**) and (b) P6HexPy obtained after treatment of the polymerization mixture with H₂SO₄ (1 M) in air (**polymer-2**).

for C₁₂H₁₂Cl₂N₄O₄: M = 346.0236. The molecular structure of **3b** is given in the supporting data.

3-Chloro-1,4-dimethylpyrazole, the hydrolysis product of **2b**, was prepared by reacting **2b** (0.45 g, 1.0 mmol) with hydrochloric acid (12 M, 1 mL) in THF under N₂. After two days at room temperature, the product was obtained in 45% yield by purification with HPLC. ¹H NMR(CDCl₃) δ 2.00 (s, 3H, CH₃), 3.79 (s, 3H, CH₃), 7.12 (s, 1H, pyrazol-H). The product was volatile. EI-MS *m/z* 130 (M⁺); peak ratio (4:1) of the peaks at 130 (³⁵Cl) and 132 (³⁷Cl) agreed. 3-Chloro-4-methoxycarbonyl-1-methylpyrazole, the hydrolysis product of **2c**, was kindly donated by Nissan Chemical Industries, Ltd.

Measurements. IR and UV-vis spectra were recorded on a JASCO IR-810 spectrometer and a Shimadzu UV-3100PC spectrometer, respectively. ¹H- and ¹⁹F-NMR spectra were obtained with JEOL EX-400 and JEOL GX-270 spectrometers, respectively. GPC analysis of polypyridine was kindly carried out by Showa Denko K. K. with a Waters 150-C analyzer by using two Shodex HFIP-806M columns and hexafluoro-*i*-propanol (eluent).

X-ray Crystal Structure Analysis of 2a. **2a**: C₂₅H₁₄N₂NiF₁₀O, *M_r* = 607.08, 0.4 × 0.5 × 0.5 mm, Monoclinic, *P*2₁/*c* (No. 1), *a* = 7.420(10) Å, *b* = 23.79(3) Å, *c* = 13.64(1) Å, β = 93.67(10), *V* = 2403(5) Å³, *R* = 0.047, *R_w* = 0.047, *Z* = 4, *D_{calcd}* = 1.678 Mg m⁻³, *F*(000) = 1216.00, μ = 9.08 cm⁻¹, 2θ_{max} = 55°, No. observations (*I* > 3.00σ(*I*)) = 3595, No. of variable 352. Calculations were carried out by using the program package teXsan on a VAX-II computer. Atomic scattering factors were taken from the literature.³³ A full-matrix least-squares refinement was used for non-hydrogen atoms with anisotropic thermal parameters. Hydrogen atoms were located by assuming ideal positions and were included in the structure calculation without further refinement of the parameters. Crystallographic data have been deposited at the CCDC, 12 Union Road, Cambridge CB2 1EZ, UK and copies can be obtained on request, free of charge, by quoting the publication citation and the deposition numbers CCDC-186401. The data are also deposited as Document No. 75036 at the Office of the Editor of Bull. Chem. Soc. Jpn.

We are grateful to Dr. C.-H. Lee and Dr. B.-L. Lee of our laboratory and Dr. M. Takeuchi of Showa Denko K. K. for experimental support. This work was supported by a Grant-in-Aid from the Ministry of Education, Culture, Sports, Science and Technology, as well as by a grant from CREST.

Supporting Data:

Tables of the second-order rate constant, *k* (cf. Eq. 4), and kinetic parameters for the reductive elimination of R-R from **1** (Table S1), X-ray crystallographical data of **2b** and **3c** (Table S2), and molecular structure of **2b** (Fig. S1), and molecular structure of **3c** (Fig. S2) are deposited as Document No. 75036 at the Office of the Editor of Bull. Chem. Soc. Jpn. and are also available from the author upon request.

References

- 1 a) J. P. Collman, L. S. Hege, J. R. Norton, and R. G. Finke, "Principles and Applications of Organotransition Metal Chemistry," University Science Book, Mill Valley (1987), p. 322. b) "Comprehensive Organometallic Chemistry; Pergamon," ed by G. Wilkinson, F. A. G. Stone, and E. W. Abel, Oxford, (1982), Vol 6. c) J. K. Kochi, "Organometallic Mechanisms and Catalysis," Academic Press, New York (1978). d) A. Yamamoto, "Organotransition Metal Chemistry," John Wiley, New York (1986). e) R. H. Crabtree, "The Organometallic Chemistry of the Transition Metals," John Wiley, New York (1988).
- 2 For diorganonickel(II) complexes, e.g., a) T. Yamamoto, A. Yamamoto, and S. Ikeda, *J. Am. Chem. Soc.*, **93**, 3350 and 3360 (1971). b) T. Yamamoto, Y. Nakamura, and A. Yamamoto, *Bull. Chem. Soc. Jpn.*, **49**, 191 (1976). c) M. Uchino, K. Asagi, A. Yamamoto, and S. Ikeda, *J. Organomet. Chem.*, **84**, 93 (1975); d) B. Åkermark, H. Johansen, B. Roos, and U. Wahlgren, *J. Am.*

- Chem. Soc.*, **101**, 5876 (1979). e) P. Binger and M. Doyle, *J. Organomet. Chem.*, **162**, 195 (1978). f) M. J. Doyle, J. McMeeking, and P. Binger, *J. Chem. Soc., Chem. Commun.*, **1976**, 376. g) H. Hoberg and A. Herrera, *Angew. Chem., Int. Ed. Engl.*, **19**, 927 (1980). h) S. Komiya, Y. Abe, A. Yamamoto, and T. Yamamoto, *Organometallics*, **2**, 1466 (1983). i) T. Kohara, T. Yamamoto, and A. Yamamoto, *J. Organomet. Chem.*, **192**, 265 (1980). j) B. Åkermark and A. Ljungqvist, *J. Organomet. Chem.*, **149**, 97 (1978). k) T. Yamamoto, J. Ishizu, T. Kohara, S. Komiya, and A. Yamamoto, *J. Am. Chem. Soc.*, **102**, 3758 (1980). l) K. Tatsumi, A. Nakamura, S. Komiya, A. Yamamoto, and T. Yamamoto, *J. Am. Chem. Soc.*, **106**, 8181 (1984). m) T. Yamamoto and A. Yamamoto, *J. Organomet. Chem.*, **57**, 127 (1973). n) S. Komiya, Y. Arai, K. Tanaka, T. Yamamoto, and A. Yamamoto, *Organometallics*, **4**, 1130 (1985).
- 3 For diorganopalladium(II) complexes, e.g., a) J. F. Hartwig, S. Richards, D. Barañano, and F. Paul, *J. Am. Chem. Soc.*, **118**, 3626 (1996). b) R. A. Widenhoefer, H. A. Zhong, and S. L. Buchwald, *J. Am. Chem. Soc.*, **119**, 6787 (1997). c) F. Ozawa, K. Kurihara, T. Yamamoto, and A. Yamamoto, *Bull. Chem. Soc. Jpn.*, **58**, 399 (1985). d) K. Osakada, R. Sakata, and T. Yamamoto, *Organometallics*, **16**, 5354 (1997). e) F. Ozawa, K. Hidaka, T. Yamamoto, and A. Yamamoto, *J. Organomet. Chem.*, **330**, 253 (1987). f) T. Yamamoto, O. Saito, and A. Yamamoto, *J. Am. Chem. Soc.*, **103**, 5600 (1981).
- 4 For organoplatinum(II) complexes, e.g., a) P. S. Braterman, and R. J. Cross, G. B. Young, *J. Chem. Soc. Dalton Trans.*, **1976**, 1306 and 1310. b) D. M. Crumpton, K. I. Goldberg, *J. Am. Chem. Soc.*, **122**, 962 (2000).
- 5 Ni promoted; e.g., a) K. Tamao, K. Sumitani, and M. Kumada, *J. Am. Chem. Soc.*, **94**, 4374 (1972). b) K. Tamao, K. Sumitani, Y. Kiso, M. Zembayashi, A. Fujioka, S. Kodama, I. Nakajima, A. Minato, and M. Kumada, *Bull. Chem. Soc. Jpn.*, **49**, 1958 (1976). c) R. J. P. Corriu and J. P. Masse, *J. Chem. Soc., Chem. Commun.*, **1972**, 144. d) M. F. Semmelhack, P. M. Helquest, and L. D. Jones, *J. Am. Chem. Soc.*, **93**, 5903 (1971). e) T. Yamamoto, S. Wakabayashi, and K. Osakada, *J. Organomet. Chem.*, **428**, 223 (1992). f) J. Terao, H. Watanabe, A. Ikuma, H. Kuniyasu, and N. Kanbe, *J. Am. Chem. Soc.*, **124**, 4222 (2002) (published after submission (during revision) of this paper).
- 6 Pd promoted; e.g., a) A. Sekiya and N. Ishikawa, *J. Organomet. Chem.*, **118**, 349 (1976); b) J. K. Stille, *Angew. Chem.*, **98**, 504 (1986). c) H. A. Dieck and R. F. Heck, *J. Organomet. Chem.*, **93**, 259 (1975). d) K. Sonogashira, Y. Tohda, and N. Hagihara, *Tetrahedron Lett.*, **16**, 4467 (1975). e) N. Miyaura and A. Suzuki, *Chem. Rev.*, **95**, 2457 (1995).
- 7 a) T. Yamamoto and A. Yamamoto, *Chem. Lett.*, **1977**, 353. b) T. Yamamoto, Y. Hayashi, and A. Yamamoto, *Bull. Chem. Soc. Jpn.*, **51**, 2091 (1978). c) R. D. McCullough and R. D. Lowe, *J. Chem. Soc., Chem. Commun.*, **1992**, 70. d) T.-A. Chen and R. D. Rieke, *J. Am. Chem. Soc.*, **114**, 10087 (1992). e) J. I. Nonos, J. W. Kampf, M. D. Curtis, L. Gonzalez, and D. C. Martin, *Chem. Mater.*, **7**, 23332 (1995). f) T. Yamamoto, *Prog. Polym. Sci.*, **17**, 1153 (1992); *J. Synth. Org. Chem. Jpn.*, **53**, 999 (1995). *Bull. Chem. Soc. Jpn.*, **72**, 621 (1999), *Macromol. Rapid Commun.*, **23**, 583 (2002); *Synlett*, in press. g) S. Setayesh, A. C. Grimsdale, T. Weil, V. Enkelman, K. Müllen, F. Meghdadi, E. J. W. List, and G. Leising, *J. Am. Chem. Soc.*, **123**, 946 (2001).
- 8 Z. Bao, W. K. Chan, and L. Yu, *J. Am. Chem. Soc.*, **117**, 12426 (1995).
- 9 a) P. W. Jolly and G. Wilke, "The Organic Chemistry of Nickel," Academic Press, New York (1974). b) P. G. Cookson and G. B. Deacon, *J. Organomet. Chem.*, **33**, C38 (1971). c) Y. Murakami, and T. Yamamoto, *Inorg. Chem.*, **36**, 5682 (1997). d) T. Yamamoto and M. Abila, *J. Organomet. Chem.*, **535**, 209 (1997). e) T. Yamamoto, Y. Murakami, and M. Abila, *Chem. Lett.*, **1999**, 419. f) B. B. Anderson, C. L. Belrens, L. Radonovich, and K. J. Klabunde, *J. Am. Chem. Soc.*, **98**, 5390 (1976).
- 10 a) S. S. Stall, J. A. Labinger, and J. E. Bercaw, *J. E. J. Am. Chem. Soc.*, **117**, 9371 (1995). b) T. Yamamoto, T. Kohara, and A. Yamamoto, *Bull. Chem. Soc. Jpn.*, **54**, 1720 (1981). c) H. A. Zhong, J. A. Labinger, and J. E. Bercaw, *J. Am. Chem. Soc.*, **124**, 1378 (2002).
- 11 a) G. R. Newkome and W. W. Paudler, "Contemporary Heterocyclic Chemistry," John Wiley, New York (1982).
- 12 a) G. W. Parshall, *J. Am. Chem. Soc.*, **96**, 2360 (1974). b) B. Corain and G. Favero, *J. Chem. Soc. Dalton Trans.*, **1975**, 283. c) M. Seno, S. Tsuchiya, M. Hidai, and Y. Uchida, *Bull. Chem. Soc. Jpn.*, **49**, 1184 (1976). d) Y.-J. Kim, T. Maruyama, K. Osakada, and T. Yamamoto, *J. Chem. Soc. Dalton Trans.*, **1994**, 943. f) Z.-H. Zhou and T. Yamamoto, *J. Organomet. Chem.*, **414**, 119 (1991).
- 13 The reaction of Ni(cod)(bpy) with chlorobenzene gives [NiCl(C₆H₅)(bpy)]. Stirring [NiCl(C₆H₅)(bpy)] in THF at room temperature for a longer period (12 h) yielded biphenyl in 70% yield, instead of Ni(C₆H₅)₂(bpy). Reaction of [Ni(cod)(bpy)] with NC(C₆H₄)Cl-*p* directly gave Ar-Ar (4,4'-NC(C₆H₄)-(C₆H₄)CN) in 78% yield.
- 14 Use of other highly electron-withdrawing aromatic compounds such as 2-cyano-(3-fluoro)chlorobenzene and 2-cyano-4-(trifluoromethyl)chlorobenzene in the reaction with [Ni(cod)(bpy)] (cf. Scheme 1) also gave products whose data from elemental and ¹H-NMR analyses roughly agreed with those of [NiAr₂(bpy)]. However, isolation of the product by separating it from another disproportionation product, [NiX₂(bpy)], was not successful. The electron transfer was associated with σ(Ni-C) to d*(Ni) transition.^{2a}
- 15 J. P. Maier, and D. W. Turner, *Faraday Discuss. Chem. Soc.*, **54**, 149 (1972).
- 16 a) K. Watanabe, *J. Chem. Phys.*, **26**, 542 (1957). b) "Gmelins Handbuch der Anorganischen Chemie: Achte Völlig: Chlor: Ergänzungsband Teil B-Lieferung 1," Verlag Chemie, Weinheim (1968), p. 73.
- 17 E. M. Kosower, *J. Am. Chem. Soc.*, **80**, 3253 (1958). Energy of a CT band usually increases linearly with an increase in Z value.
- 18 M. Abila and T. Yamamoto, *J. Organomet. Chem.*, **532**, 262 (1997).
- 19 The oxidative addition of Ar-CN¹⁸ and Ar-F^{9d} bonds to a zerovalent nickel complex, Ni(bpy), is a considerably slow process. However, the reductive elimination reaction of **1a** is also slow. In the case of **1a**, isosbestic points are not observed often. This seems to be due to the simultaneous occurrence of the reductive elimination and the oxidative addition with comparable reaction rates. Even in this case, the reductive elimination can be followed by the decrease in the absorbance of the absorption peak A of **1a** at 15800 cm⁻¹.
- 20 R. W. Jr. Taft, *J. Am. Chem. Soc.*, **75**, 4231 (1953).
- 21 A. Carrington and A. D. McLachlan, "Introduction to Magnetic Resonance with Applications to Chemistry and Physical Chemistry," Harper & Row, New York (1967).
- 22 K. J. Klabunde, B. B. Anderson, M. Badar, and L. J.

Radonovich, *J. Am. Chem. Soc.*, **100**, 1313 (1978).

23 L. J. Radonovich, F. J. Koch, and T. A. Albright, *Inorg. Chem.*, **19**, 3373 (1980).

24 "Comprehensive Inorganic Chemistry," ed by J. C. Bailar H. J. Emeleus, R. Nyholm, A. F. Trotman-Dichenson, Pergamon, Oxford (1973), Vol. 2, p. 1325.

25 C. A. Tolman, *J. Am. Chem. Soc.*, **92**, 4217 (1970).

26 K. Izutsu, "Acid-Base Dissociation Constants in Dipolar Aprotic Solvents," Blackwell Sci., New York (1990). For example H_2SO_4 has $\text{p}K_{\text{a}}(1)$ and $\text{p}K_{\text{a}}(2)$ values of 1.4 and 14.7 for the first-step dissociation and second-step dissociation in DMSO, respectively.

27 E. Wilhelm and R. Battino, *Chem. Rev.*, **73**, 1 (1973).

28 M. H. Gubelmann and A. F. Williams, *Struct. Bonding*

(Berlin), **55**, 1 (1983).

29 T. Yamamoto, T. Maruyama, Z.-H. Zhou, T. Ito, T. Fukuda, Y. Yoneda, F. Begum, T. Ikeda, S. Sasaki, H. Takezoe, A. Fukuda, and K. Kubota, *J. Am. Chem. Soc.*, **116**, 4832 (1994).

30 T. Yamamoto and H. Etori, *Macromolecules*, **28**, 3371 (1995).

31 D. D. Gebler, Y. Z. Wang, and J. W. Blatchford, S. W. Jessen, L.-B. Lin, T. L. Gustafson, H. L. Wang, T. M. Swager, A. G. MacDiarmid, and A. J. Epstein, *J. Appl. Phys.*, **78**, 4264 (1995).

32 B. Bogdanovic, M. Kroner, and G. Wilke, *Ann. Chem.*, **1**, 699 (1966).

33 "International Tables for X-ray Crystallography," Kynoch, Birmingham, England (1974), Vol. IV.